

Angle-Dependent van Hove Singularities in a Slightly Twisted Graphene Bilayer

Wei Yan,¹ Mengxi Liu,² Rui-Fen Dou,¹ Lan Meng,¹ Lei Feng,¹ Zhao-Dong Chu,¹ Yanfeng Zhang,^{2,3,*}
Zhongfan Liu,² Jia-Cai Nie,¹ and Lin He^{1,†}

¹Department of Physics, Beijing Normal University, Beijing 100875, People's Republic of China

²Center for Nanochemistry (CNC), College of Chemistry and Molecular Engineering, Peking University, Beijing 100871, People's Republic of China

³Department of Materials Science and Engineering, College of Engineering, Peking University, Beijing 100871, People's Republic of China

(Received 29 April 2012; published 17 September 2012)

Recent studies show that two low-energy van Hove singularities (VHSs) seen as two pronounced peaks in the density of states could be induced in a twisted graphene bilayer. Here, we report angle-dependent VHSs of a slightly twisted graphene bilayer studied by scanning tunneling microscopy and spectroscopy. We show that energy difference of the two VHSs follows $\Delta E_{\text{vhs}} \sim \hbar v_F \Delta K$ between 1.0° and 3.0° [here $v_F \sim 1.1 \times 10^6$ m/s is the Fermi velocity of monolayer graphene, and $\Delta K = 2K \sin(\theta/2)$ is the shift between the corresponding Dirac points of the twisted graphene bilayer]. This result indicates that the rotation angle between graphene sheets does not result in a significant reduction of the Fermi velocity, which quite differs from that predicted by band structure calculations. However, around a twisted angle $\theta \sim 1.3^\circ$, the observed $\Delta E_{\text{vhs}} \sim 0.11$ eV is much smaller than the expected value $\hbar v_F \Delta K \sim 0.28$ eV at 1.3° . The origin of the reduction of ΔE_{vhs} at 1.3° is discussed.

DOI: [10.1103/PhysRevLett.109.126801](https://doi.org/10.1103/PhysRevLett.109.126801)

PACS numbers: 73.22.Pr, 68.37.Hk, 73.21.Ac

Graphene, a two-dimensional honeycomb lattice of carbon atoms, is considered a strong candidate for post-silicon electronic devices [1–7]. Its topological features of the electronic states can be changed by lattice deformations [8–13]. This is of fundamental importance in providing building blocks and device concepts for an all-graphene circuit in the future. Compared with single-layer graphene, graphene bilayer displays even more complex electronic band structures and intriguing properties [14–30]. Recent studies reveal that the low-energy band structure of a graphene bilayer is extremely sensitive to the stacking sequence [14,18]. Two low-energy van Hove singularities (VHSs), which originate from the two saddle points in the band structure, were observed in the twisted graphene bilayer as two pronounced peaks in the density of states (DOS) [25,30]. Li *et al.* studied the VHSs of a graphene bilayer [a chemical vapor deposition (CVD)-grown graphene monolayer deposited on a graphite surface] with three different twisted angles by scanning tunneling microscopy and spectroscopy (STM and STS). They demonstrated that the energy difference of the two VHSs shows a strong angle dependence [25]. After this seminal observation, several authors addressed the physics of a twisted graphene bilayer theoretically and obtained many interesting results [31–40]. The most striking results are the significant angle-dependent reduction of the Fermi velocity and the appearance of almost dispersionless bands (flat bands) around $1^\circ \sim 1.5^\circ$ [32,33,35,37–39]. It suggests that electrons in a graphene bilayer can be changed from ballistic to localized by simply varying the rotation angle. However, a systematic experimental study of twisted

angle-dependent band structures in a graphene bilayer is still scarce so far.

In this Letter, we address the twisted angle-dependent VHSs in a graphene bilayer (with twisted angle $< 3.0^\circ$). The morphology and local DOS of the graphene bilayer with as many as eight different twisted angles were studied by STM and STS, respectively. The energy difference of the two VHSs increases linear with the sine of twisted angle, i.e., $\Delta E_{\text{vhs}} \sim \hbar v_F \Delta K$, between 1.0° and 3.0° . Here $v_F \sim 1.1 \times 10^6$ m/s, $\Delta K = 2K \sin(\theta/2)$, the shift between the corresponding Dirac points of the twisted graphene bilayer, and $K = 4\pi/3a$ ($a \sim 0.246$ nm is the lattice constant of the hexagonal lattice). Our result indicates that the rotation angle between graphene sheets do not result in the reduction of the Fermi velocity. This differs much from that predicted by previous theories.

The graphene bilayer was grown on a $25 \mu\text{m}$ thin polycrystalline Rh foil via a traditional ambient pressure CVD method. The process is similar to the synthesis of graphene on Pt and Cu foils, which were reported in previous papers [41,42]. The details of the synthesis of the sample is described in the Supplemental Material [43]. The thickness of the as-grown graphene was characterized by Raman spectra measurements (see Fig. S1 in the Supplemental Material [43]), as reported in our previous papers [41,42]. The STM system was an ultrahigh vacuum four-probe scanning probe microscope from UNISOKU. All STM and STS measurements were performed at liquid-nitrogen temperature and the images were taken in a constant-current scanning mode. The STM tips were obtained by a chemical etching from a wire of Pt(80%) Ir(20%) alloys.

Lateral dimensions observed in the STM images were calibrated using a standard graphene lattice. The STS spectrum, i.e., the dI/dV - V curve, was carried out with a standard lock-in technique using a 957 Hz alternating current modulation of the bias voltage.

Figure 1(a) shows a large-area STM image of the graphene grown on polycrystalline Rh foil taken from a flat terrace of the Rh surface (see Fig. S2 in the Supplemental Material [43] for a larger STM image). Clear periodic protuberances with a period of 4.9 nm are observed, as shown in Fig. 1(b). The periodic protuberances are attributed to the moiré pattern arising from a stacking misorientation between the top graphene layer and the underlying layer. The twisted angle θ is related to the period of the moiré pattern by $D = a/[2 \sin(\theta/2)]$ and is estimated as 2.9° . For monolayer graphene on a (111) surface of single-crystal Rh, the lattice mismatch between graphene (0.246 nm) and Rh(111) (0.269 nm) and the strong C-Rh covalent bond also lead to hexagonal moiré superstructures. However, the expected periodicity is only about 2.9 nm resulting from a 12C/11Rh coincidence lattice [44–46] (see Fig. S3 in the supplemental material [43] for STM images of monolayer graphene on a (111) surface of single-crystal Rh.). The smallest period of the moiré pattern studied in this Letter is about 4.9 nm (corresponding to the twisted angle 2.9°). This eliminates the lattice mismatch of monolayer graphene and Rh(111) as the origin of the observed periodic protuberances. Additionally, for monolayer graphene grown on

polycrystalline Rh foil, the coupling between graphene and the substrate is much weaker than that of monolayer graphene on a single-crystal Rh and the coupling strength varies on different monolayer graphene (see Fig. S4 in the Supplemental Material [43] for two typical STS curves recorded on two different monolayer graphene on polycrystalline Rh foil). Because of the weak coupling, no periodic moiré superstructures can be seen in monolayer graphene grown on polycrystalline Rh foil.

Figures 1(c) and 1(d) show the atomic-resolution STM images of the graphene. In the twisted graphene bilayer, there are local Bernal-stacked regions, where a triangular lattice is expected to be seen [47]. However, only a honeycomb lattice can be observed in the atomic-resolution STM image of the sample both on and between the protuberances, as shown in Fig. 1(d). In the literature [47,48], many groups have reported both the triangular and the honeycomb lattice in graphite with a Bernal-stacked lattice. The exact origin of this phenomenon is still not clear, as discussed in Ref. [47].

A graphene bilayer with different twisted angles can be observed on the graphene samples grown on Rh foils. Figure 2 shows six typical STM topographs of a graphene bilayer with different stacking misorientation angles. These systems provide an ideal platform to study the twisted angle-dependent VHSs. For a twisted graphene bilayer, the Dirac points of the two layers no longer coincide and the zero-energy states occur at $k = -\Delta K/2$ in layer 1 and $k = \Delta K/2$ in layer 2. The displaced Dirac cones cross at energies $\pm \hbar v_F \Delta K/2$ and two saddle points are unavoidable along the intersection of the two cones when there is a finite interlayer hopping [18].

Figures 3(a) and 3(b) show the STM image and STS spectra of a graphene bilayer with a twisted angle $\sim 1.1^\circ$, respectively. Although the peak heights and degree of

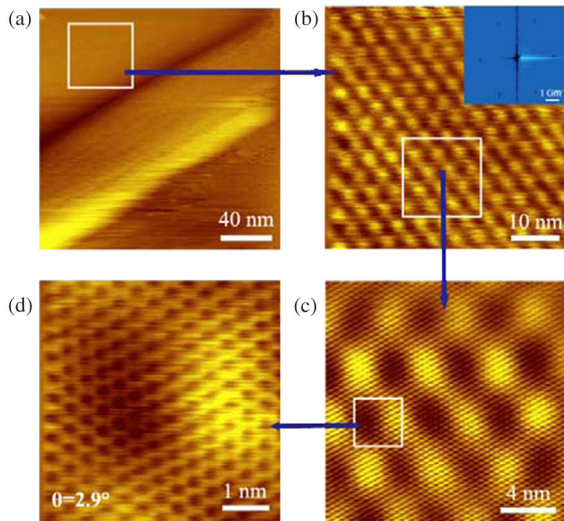


FIG. 1 (color online). (a) A $200 \times 200 \text{ nm}^2$ STM image of graphene on Rh foil ($V_{\text{sample}} = -600 \text{ mV}$ and $I = 0.34 \text{ nA}$). (b) Zoom-in topography of the white frame in (a) shows a moiré pattern with a period of 4.9 nm ($V_{\text{sample}} = -280 \text{ mV}$ and $I = 0.06 \text{ nA}$). The inset shows Fourier transforms of the superstructures. (c) Zoom-in image of white frame in panel (b) ($V_{\text{sample}} = -351 \text{ mV}$ and $I = 0.14 \text{ nA}$). (d) Atomic-resolution image of the white frame in panel (c) ($V_{\text{sample}} = -496 \text{ mV}$ and $I = 0.17 \text{ nA}$). The twisted angle of the graphene bilayer is estimated as about 2.9° .

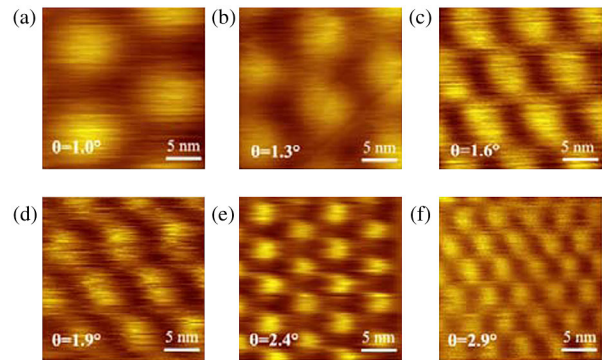


FIG. 2 (color online). (a)–(f) The $22 \times 22 \text{ nm}$ STM topographs of graphene bilayer with six different twisted angles. The period of the moiré pattern changes as a function of the twisted angle θ . (a) $\theta = 1.0^\circ$, $D = 14.1 \text{ nm}$, $V_{\text{sample}} = 317 \text{ mV}$, $I = 0.47 \text{ nA}$. (b) $\theta = 1.3^\circ$, $D = 10.8 \text{ nm}$, $V_{\text{sample}} = 560 \text{ mV}$, $I = 0.33 \text{ nA}$. (c) $\theta = 1.6^\circ$, $D = 8.8 \text{ nm}$, $V_{\text{sample}} = 246 \text{ mV}$, $I = 0.88 \text{ nA}$. (d) $\theta = 1.9^\circ$, $D = 7.4 \text{ nm}$, $V_{\text{sample}} = -375 \text{ mV}$, $I = 0.11 \text{ nA}$. (e) $\theta = 2.4^\circ$, $D = 5.8 \text{ nm}$, $V_{\text{sample}} = -304 \text{ mV}$, $I = 0.34 \text{ nA}$. (f) $\theta = 2.9^\circ$, $D = 4.9 \text{ nm}$, $V_{\text{sample}} = -600 \text{ mV}$, $I = 0.17 \text{ nA}$.

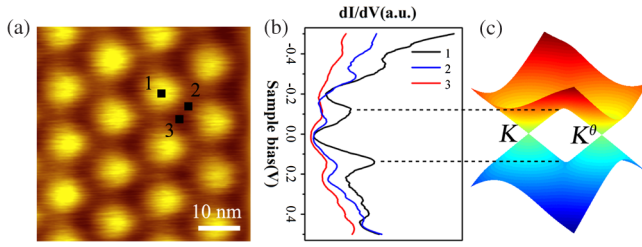


FIG. 3 (color online). (a) A typical STM image of a graphene bilayer with the twisted angle $\sim 1.1^\circ$ ($V_{\text{sample}} = -317$ mV and $I = 0.47$ nA). The period of the moiré pattern is about 12.8 nm. (b) Tunneling spectra recorded on bright and dark regions of the moiré pattern at positions indicated in panel (a). The spectra show two peaks attributed to two van Hove singularities. (c) Electronic band structure of the twisted graphene bilayer with a finite interlayer coupling. Two saddle points (VHSs) form at $k = 0$ between the two Dirac cones, K and K_θ , with a separation of $\Delta K = 2K \sin(\theta/2)$. The low-energy VHSs contribute to two pronounced peaks flanking a zero bias in the tunneling spectra.

asymmetry of the spectra depend on their positions in the moiré pattern (bright or dark regions in Fig. 3(a)), all STS spectra show two peaks flanking zero-bias, as shown in Fig. 3(b). Similar position dependent spectra were also observed in the moiré pattern of the CVD-grown graphene deposited on a graphite surface [25]. The tunneling spectrum gives direct access to the local DOS of the surface at the position of the STM tip. The two peaks in the tunneling spectra are attributed to the two van Hove peaks in DOS, which originate from the two saddle points of the band structure, as shown in Fig. 3(c) (see Fig. S5 and the Supplemental Material [43] for details of the analysis).

Figure 4 shows eight typical tunneling curves taken on a graphene bilayer with different twisted angles. In order to ascertain the reproducibility of the results, several tens of tunneling spectra on different positions of the graphene bilayer with different twisted angles are recorded. Although the peak heights and peak positions of the spectra vary slightly, the main features of these dI/dV - V curves are almost completely reproducible (for example, see Fig. S6 of the Supplemental Material [43] for more STS spectra). Obviously, the two VHSs of these samples show a strong angle-dependent energy difference. At a twisted angle $\theta \sim 1.3^\circ$, the two tunneling peaks show the least energy difference, which will be discussed subsequently. Additionally, the positions of the two VHSs are not always symmetric around the Fermi level, suggesting charge transfer between the graphene and the substrate. The magnitude of the charge transfer should mainly depend on the coupling strength between the sublayer graphene and the substrate, which varies in different samples (see Fig. S4 in the Supplemental Material [43]).

Figure 5 summarizes the energy difference of the two VHSs ΔE_{vhs} as a function of the twisted angles (see Fig. S7 of the Supplemental Material [43] for methods to choose the positions of VHSs). Except at 1.3° , ΔE_{vhs} increase

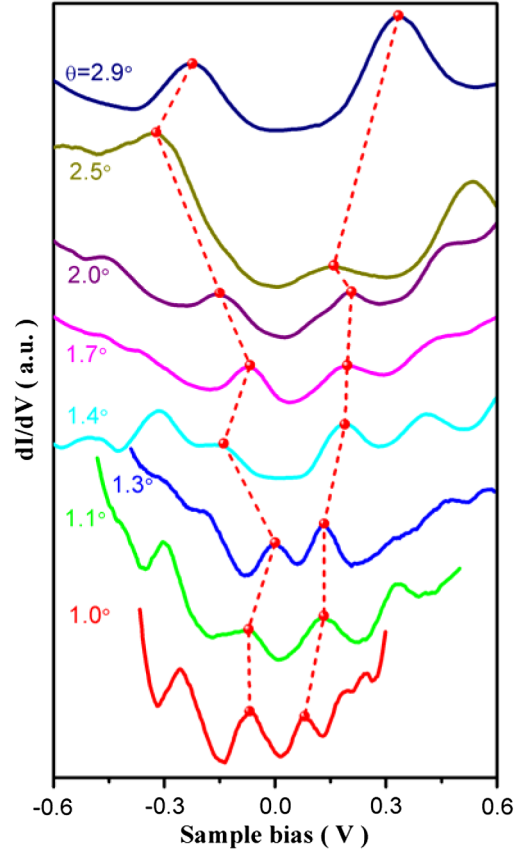


FIG. 4 (color online). Eight dI/dV - V curves taken on a graphene bilayer with different twisted angles. The center of the two peaks flanking a zero bias, which originate from the two van Hove peaks of local density of states, are indicated by red solid dots.

linearly with the sine of the twisted angle (or the twisted angle for small angles). Theoretically, it is predicted that the position of the two VHSs can be simply estimated by $\Delta E_{\text{vhs}} = \hbar v_F' \Delta K - 2t_\theta$ [25,33,37]. Here, t_θ is the interlayer hopping parameter and v_F' is the renormalized Fermi velocity of the graphene bilayer. While assuming t_θ is a constant that is independent of the twisted angle, the value of ΔE_{vhs} is expected to increase linearly with the twisted angle. Li *et al.* studied the VHSs of the CVD-grown graphene monolayer deposited on graphite with three different twisted angles and reported this linear dependence (in their experiment, $2t_\theta \sim 0.216$ eV is obtained) [25]. Their result is also plotted along with our experimental data in Fig. 5. An obvious deviation between our experimental result and their data is observed.

Our experimental result reveals that the energy difference of the two VHSs follows $\Delta E_{\text{vhs}} \sim \hbar v_F \Delta K$ between 1.0° and 3.0° except at 1.3° , where $v_F \sim 1.1 \times 10^6$ m/s. It suggests that the displaced Dirac cones of a slightly twisted graphene bilayer cross and two saddle points are formed along the intersection of the two cones at energies about $\pm \hbar v_F \Delta K / 2$. This indicates that the rotation angle between graphene sheets does not result in a significant reduction of the Fermi velocity. In the literature, Landau-level

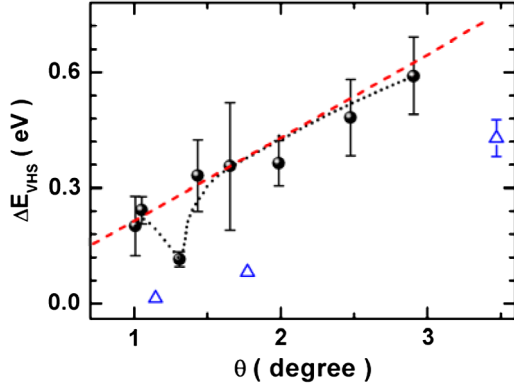


FIG. 5 (color online). The energy difference of the two VHS ΔE_{vhs} as a function of the twisted angles. The solid black circles are the average experimentally measured values obtained from several tens of tunneling spectra for each twisted angle and the error bars in energy represent the minimum and maximum observed energies of ΔE_{vhs} . The open triangles are the experimental results taken from the CVD-grown graphene sheet deposited on graphite, as reported in [25]. The red dashed line is plotted according $\Delta E_{\text{vhs}} = \hbar v_F \Delta K$, where $v_F \sim 1.1 \times 10^6$ m/s, $\Delta K = 2K \sin(\theta/2)$. The black dotted curve is the guide to eyes.

spectroscopy of a twisted graphene bilayer demonstrated a negligible renormalization of the Fermi velocity [49]. Hicks *et al.* measured the band structure of a slightly twisted graphene bilayer with $\theta \sim 1.7^\circ$, 2.4° , and 4.2° by using angle-resolved photoemission and also did not detect any significant change of the Fermi velocity [27]. Very recently, the problem regarding the Fermi velocity of the slightly twisted graphene bilayer is discussed theoretically and two distinct electronic states of this coupled system are predicted to account for the two distinct results [50]. In Refs. [25,26], the experiment was carried out on a CVD-grown graphene monolayer deposited on graphite and the top layer of graphite was considered as an isolated monolayer graphene. In fact, there is strong coupling between the top layer and the deeper layers below the graphite surface. The electronic band structure of graphite differs quite a bit from that of monolayer graphene. This may be the origin of the observed reduction of Fermi velocity in [25,26].

The large deviation of ΔE_{vhs} between our experimental result and the data in Ref. [25] mainly arises from the magnitude of the interlayer hopping parameter. In their experiment, $2t_\theta \sim 0.216$ eV is obtained to account for the experimental result. In our experiment, the two saddle points appear at energies about $\pm \hbar v_F \Delta K/2$, which suggests that the magnitude of t_θ is negligible compared with $\hbar v_F \Delta K$ (it is interesting to note that although the magnitude of t_θ is negligible in our system, it still results in two saddle points that lead to two VHSs in DOS). The effect of the substrate may be the possible origin of the different interlayer hopping. Further experiments carried out on a graphene bilayer grown on different substrates are expected to uncover the exact nature of this difference.

Additionally, the abrupt reduction of ΔE_{vhs} at $\theta \sim 1.3^\circ$ observed in our experiment is very interesting. The observed $\Delta E_{\text{vhs}} \sim 0.11$ eV is much less than the expected value $\hbar v_F \Delta K \sim 0.28$ eV at 1.3° . There are two possible origins for this observation. The first one is that some unknown effects enhance the interlayer coupling strength at $\theta \sim 1.3^\circ$, resulting in a small ΔE_{vhs} . The second nontrivial one is that there are flat bands in twisted the graphene bilayer with a twisted angle around 1.3° and the reduction of Fermi velocity around 1.3° leads to the small ΔE_{vhs} . If this is the case, then the abrupt reduction of ΔE_{vhs} at $\theta \sim 1.3^\circ$ is beyond the description of any continuum model [32,33,35,37–39]. A resolution of this issue requires further theoretical analysis and experiments. Very recently, two theoretical studies suggest that superconductivity could be induced in graphene by involving repulsive electron-electron interactions [51,52]. One possible approach is to raise the Fermi level up to the vicinity of a saddle point in graphene's electronic structure [52]. This is very difficult to achieve in monolayer graphene, but to some extent easy to realize in a twisted graphene bilayer, in which the saddle point is located not far from the Fermi level, as shown in Fig. 4. For the twisted graphene bilayer with $\theta \sim 1.3^\circ$, one saddle point is naturally placed at the Fermi energy, as shown in Figure 4 and Fig. S6 [43]. Further experiments will be carried out to explore the novel superconductivity in a graphene bilayer.

In summary, we address the twisted angle-dependent VHSs in a graphene bilayer grown on Rh foil. The energy difference of the two VHSs follows $\Delta E_{\text{vhs}} \sim \hbar v_F \Delta K$, between 1.0° and 3.0° . Our result indicates that the rotation angle between graphene sheets does not result in a significant reduction of the Fermi velocity. The experimental results reported here suggest that the graphene bilayer grown on Rh foil provides an ideal platform for VHSs engineering of electronic properties and exploring many attractive phases.

This work was supported by the National Natural Science Foundation of China (Grants No. 11004010, No. 10804010, No. 10974019, No. 21073003, No. 51172029, and No. 91121012), the Fundamental Research Funds for the Central Universities, and the Ministry of Science and Technology of China (Grants No. 2011CB921903, No. 2012CB921404, No. 2013CB921701). W.Y. and M.L. contributed equally to this work.

*yanfengzhang@pku.edu.cn

†helin@bnu.edu.cn

- [1] K. S. Novoselov, A. K. Geim, S. V. Morozov, D. Jiang, Y. Zhang, S. V. Dubonos, I. V. Grigorieva, and A. A. Firsov, *Science* **306**, 666 (2004).
- [2] A. K. Geim and K. S. Novoselov, *Nature Mater.* **6**, 183 (2007).

- [3] A. H. Castro Neto, F. Guinea, N. M. R. Peres, K. S. Novoselov, and A. K. Geim, *Rev. Mod. Phys.* **81**, 109 (2009).
- [4] S. Das Sarma, S. Adam, E. H. Hwang, and E. Rossi, *Rev. Mod. Phys.* **83**, 407 (2011).
- [5] K. S. Novoselov, A. K. Geim, S. V. Morozov, D. Jiang, M. I. Katsnelson, I. V. Grigorieva, S. V. Dubonos, and A. A. Firsov, *Nature (London)* **438**, 197 (2005).
- [6] Y. B. Zhang, Y. W. Tan, H. L. Stormer, and P. Kim, *Nature (London)* **438**, 201 (2005).
- [7] M. O. Goerbig, *Rev. Mod. Phys.* **83**, 1193 (2011).
- [8] N. Levy, S. A. Burke, K. L. Meaker, M. Panlasigui, A. Zettl, F. Guinea, A. H. Castro Neto, and M. F. Crommie, *Science* **329**, 544 (2010).
- [9] H. Yan, Y. Sun, L. He, J. C. Nie, and M. H. W. Chan, *Phys. Rev. B* **85**, 035422 (2012).
- [10] M. M. Ugeda, I. Brihuega, F. Guinea, and J. M. Gomez-Rodriguez, *Phys. Rev. Lett.* **104**, 096804 (2010).
- [11] M. M. Ugeda, D. Fernandez-Torre, I. Brihuega, P. Pou, A. J. Martinez-Galera, R. Perez, and J. M. Gomez-Rodriguez, *Phys. Rev. Lett.* **107**, 116803 (2011).
- [12] L. Tarruell, D. Greif, T. Uehlinger, G. Jotzu, and T. Esslinger, *Nature (London)* **483**, 302 (2012).
- [13] K. K. Gomes, W. Mar, W. Ko, F. Guinea, and H. C. Manoharan, *Nature (London)* **483**, 306 (2012).
- [14] E. McCann and V. I. Falko, *Phys. Rev. Lett.* **96**, 086805 (2006).
- [15] K. S. Novoselov, E. McCann, S. V. Morozov, V. I. Falko, M. I. Katsnelson, U. Zeitler, D. Jiang, F. Schedin, and A. K. Geim, *Nature Phys.* **2**, 177 (2006).
- [16] G. M. Rutter, S. Jung, N. N. Klimov, D. B. Newell, N. B. Zhitenev, and J. A. Stroscio, *Nature Phys.* **7**, 649 (2011).
- [17] Z. Q. Li, E. A. Henriksen, Z. Jiang, Z. Hao, M. C. Martin, P. Kim, H. L. Stormer, and D. N. Basov, *Phys. Rev. Lett.* **102**, 037403 (2009).
- [18] J. M. B. Lopes dos Santos, N. M. R. Peres, and A. H. Castro Neto, *Phys. Rev. Lett.* **99**, 256802 (2007).
- [19] S. Kim, K. Lee, and E. Tutuc, *Phys. Rev. Lett.* **107**, 016803 (2011).
- [20] M. Killi, S. Wu, and A. Paramekanti, *Phys. Rev. Lett.* **107**, 086801 (2011).
- [21] R. Nandkishore and L. Levitov, *Phys. Rev. Lett.* **107**, 097402 (2011).
- [22] N. Gu, M. Rudner, and L. Levitov, *Phys. Rev. Lett.* **107**, 156603 (2011).
- [23] D. S. Lee, C. Riedl, T. Beringer, A. H. Castro Neto, K. von Klitzing, U. Starke, and Jurgen H. Smet, *Phys. Rev. Lett.* **107**, 216602 (2011).
- [24] A. S. Mayorov, D. C. Elias, M. Mucha-Kruczynski, R. V. Gorbachev, T. Tudorovskiy, A. Zhukov, S. V. Morozov, M. I. Katsnelson, V. I. Falko, A. K. Geim, and K. S. Novoselov, *Science* **333**, 860 (2011).
- [25] G. H. Li, A. Luican, J. M. B. Lopes dos Santos, A. H. Castro Neto, A. Reina, J. Kong, and E. Y. Andrei, *Nature Phys.* **6**, 109 (2009).
- [26] A. Luican, G. H. Li, A. Reina, J. Kong, R. R. Nair, K. S. Novoselov, A. K. Geim, and E. Y. Andrei, *Phys. Rev. Lett.* **106**, 126802 (2011).
- [27] J. Hicks, M. Sprinkle, K. Shepperd, F. Wang, A. Tejada, A. Taleb-Ibrahimi, F. Bertran, P. Le Fevre, W. A. de Heer, C. Berger, and E. H. Conrad, *Phys. Rev. B* **83**, 205403 (2011).
- [28] D. L. Miller, K. D. Kubista, G. M. Rutter, M. Ruan, W. A. de Heer, M. Kindermann, P. N. First, and J. A. Stroscio, *Nature Phys.* **6**, 811 (2010).
- [29] G. M. Rutter, S. Jung, N. N. Klimov, D. B. Newell, N. B. Zhitenev, and J. A. Stroscio, *Nature Phys.* **7**, 649 (2011).
- [30] L. Meng, Z.-D. Chu, Y. Zhang, J.-Y. Yang, R.-F. Dou, J.-C. Nie, and L. He, *Phys. Rev. B* **85**, 235453 (2012).
- [31] R. de Gail, M. O. Goerbig, F. Guinea, G. Montambaux, and A. H. Castro Neto, *Phys. Rev. B* **84**, 045436 (2011).
- [32] E. Suarez Morell, J. D. Correa, P. Vargas, M. Pacheco, and Z. Barticevic, *Phys. Rev. B* **82**, 121407(R) (2010).
- [33] R. Bistritzer and Allan H. MacDonald, *Proc. Natl. Acad. Sci. U.S.A.* **108**, 12233 (2011).
- [34] S. Shallcross, S. Sharma, E. Kandelaki, and O. A. Pankratov, *Phys. Rev. B* **81**, 165105 (2010).
- [35] G. T. de Laissardiere, D. Mayou, and L. Magaud, *Nano Lett.* **10**, 804 (2010).
- [36] R. Bistritzer and A. H. MacDonald, *Phys. Rev. B* **84**, 035440 (2011).
- [37] J. M. B. Lopes dos Santos, N. M. R. Peres, and A. H. Castro Neto, [arXiv:1202.1088](https://arxiv.org/abs/1202.1088).
- [38] G. T. de Laissardiere, D. Mayou, and L. Magaud, [arXiv:1203.3144](https://arxiv.org/abs/1203.3144).
- [39] P. Moon and M. Koshino, *Phys. Rev. B* **85**, 195458 (2012).
- [40] M. Kindermann and P. N. First, *J. Phys. D* **45**, 154005 (2012).
- [41] T. Gao, S. Xie, Y. Gao, M. Liu, Y. Chen, Y. Zhang, and Z. Liu, *ACS Nano* **5**, 9194 (2011).
- [42] Y. Zhang, T. Gao, Y. Gao, S. Xie, Q. Ji, K. Yan, H. Peng, and Z. Liu, *ACS Nano* **5**, 4014 (2011).
- [43] See Supplemental Material at <http://link.aps.org/supplemental/10.1103/PhysRevLett.109.126801> for Raman spectra, more STM images, STS spectra, and the detail of the analysis.
- [44] B. Wang, M. Caffio, C. Bromley, H. Fruchtl, and R. Schaub, *ACS Nano* **4**, 5773 (2010).
- [45] M. Sicot, S. Bouvron, O. Zander, U. Rudiger, Yu. S. Dedkov, and M. Fonin, *Appl. Phys. Lett.* **96**, 093115 (2010).
- [46] M. Sicot, P. Leicht, A. Zusan, S. Bouvron, O. Zander, M. Weser, Y. S. Dedkov, K. Horn, and M. Fonin, *ACS Nano* **6**, 151 (2012).
- [47] E. Y. Andrei, G. Li, and X. Du, *Rep. Prog. Phys.* **75**, 056501 (2012).
- [48] P. Moriarty and G. Hughes, *Appl. Phys. Lett.* **60**, 2338 (1992); P. J. Ouseph, T. Poothackanal, and G. Mathew, *Phys. Lett. A* **205**, 65 (1995); J. I. Paredes, A. M. Alonso, and J. M. D. Tascon, *Carbon* **39**, 476 (2001); S. Hembacher, F. Giessibl, J. Mannhart, and C. F. Quate, *Proc. Natl. Acad. Sci. U.S.A.* **100**, 12539 (2003); H. A. Mizes, S.-i. Park, and W. A. Harrison, *Phys. Rev. B* **36**, 4491 (1987); F. Atamny, O. Spillecke, and R. Schlogl, *Phys. Chem. Chem. Phys.* **1**, 4113 (1999); Y. Wang, Y. Ye, and K. Wu, *Surf. Sci.* **600**, 729 (2006); P. Xu, Y. Yang, S. D. Barber, M. L. Ackerman, J. K. Scholz, I. A. Kornev, S. Barraza-Lopez, L. Bellaiche, and P. M. Thibado, *Phys. Rev. B* **84**, 161409 (2011).
- [49] D. M. Miller, K. D. Kubista, G. M. Rutter, W. A. de Heer, P. N. First, and J. A. Stroscio, *Science* **324**, 924 (2009).
- [50] E. J. Mele, *Phys. Rev. B* **84**, 235439 (2011).
- [51] M. V. Hosseini and M. Zareyan, *Phys. Rev. Lett.* **108**, 147001 (2012).
- [52] R. Nandkishore, L. S. Levitov, and A. V. Chubukov, *Nature Phys.* **8**, 158 (2012).